The Kinetic Mechanism of Manganese-Containing Superoxide Dismutase from *Deinococcus radiodurans*: A Specialized Enzyme for the Elimination of High Superoxide Concentrations†

Isabel A. Abreu,‡ Amy Hearn,§ Haiqain An,§ Harry S. Nick,§ David N. Silverman,§ and Diane E. Cabelli*,‡

Chemistry Department, Brookhaven National Laboratory, Building 555, Upton, New York 11973-5000, and Department of Pharmacology, University of Florida, Gainesville, Florida 32610

Received August 10, 2007; Revised Manuscript Received December 13, 2007

ABSTRACT: *Deinococcus radiodurans* (*Drad*), a bacterium with an extraordinary capacity to tolerate high levels of ionizing radiation, produces only a manganese-containing superoxide dismutase (MnSOD). As MnSOD has been shown to remove superoxide radical with varying efficiency depending upon its cellular origin, a comparison of the *Drad* MnSOD efficiency with that of both human and *Escherichia coli* MnSODs was undertaken. Pulse radiolysis studies demonstrate that, under identical ratios of enzyme to superoxide radical, the dismutation efficiencies scaled as *Drad* MnSOD > *E. coli* MnSOD > human MnSOD. Further, *Drad* MnSOD is most effective at high superoxide fluxes found under conditions of high radioactivity. A mechanism is postulated to account for the differences in the activities of the MnSODs that considers the release of peroxide as not always an optimal process.

Deinococcus radiodurans (*Drad*[1]) is a non-spore-forming bacterium with an extraordinary capacity to tolerate high levels of DNA damaging agents such as ionizing and ultraviolet radiation, and desiccation (*1*). This characteristic makes it a target organism for bioremediation processes and led to its priority in genetic sequencing (*2*). The mechanisms for such resistance have been a subject of extensive research during the past decade. In particular, its unusual DNA packaging, leading to redundancy of DNA, was postulated to be linked to the radiation resistance (*3*), but this has been the core of some controversy (*4*, *5*). Another study showed very high levels of manganese(II) not bound in any enzymatic system present in *Drad* and associated with γ radiation resistance (*6*, *7*). The authors postulated an antioxidant role for the manganese as a potential mechanism (*6*). The authors of a recent publication have suggested that a process they call "extended synthesis-dependent strand annealing" can account for the massive repair of the broken DNA that results from both desiccation and exposure to high radiation fields (*8*). Some new systems have been found that are involved in DNA repair (*9*−*15*). Additionally, a so far unique gene involved in the regulation of *recA* and *pprA* genes has been identified (*9*, *15*) in *Drad* and proposed to be involved in the regulation of oxidative stress response enzymes as it was shown that strains lacking it have reduced catalase activity (*15*). Interestingly, catalase A mutants of *Drad* do not show significantly increased sensitivity to ionizing radiation, an observation that the authors attribute to the coexistence of an active catalase B in *Drad* cellular extracts (*16*). In contrast, mutants lacking manganese superoxide dismutase (MnSOD) were shown to be more sensitive to ionizing radiation (*17*), an observation that led us to interrogate the mechanism of superoxide (O_2^-) dismutation in this MnSOD.

MnSOD is present in the cytoplasm of many prokaryotic organisms and in the mitochondria of eukaryotic cells where the majority of reactive oxygen species are formed. Apparently in *Drad* it is the sole active SOD (*17*−*20*). Classically, enzymatic O_2^- dismutation is accomplished through the diffusion controlled cycling between the oxidized and reduced forms of the enzyme upon reduction and oxidation of O_2^- to H_2O_2 and O_2 respectively; reactions 1 and 2. Diffusion controlled dismutation of superoxide is very well established for SOD1, the copper,zinc superoxide dismutases found in the cytosol of eukaryotes.

$$M^{n+}SOD + O_2^- \rightarrow M^{(n-1)+}SOD + O_2 \quad (1)$$

$$M^{(n-1)+}SOD + O_2^- (+2H^+) \rightarrow M^{n+}SOD + H_2O_2 \quad (2)$$

A modification of this overall mechanism is seen for SOD2, MnSOD, where reoxidation of the reduced $Mn^{II}SOD$ by superoxide has been shown to occur by two concomitant pathways. The proposed mechanism for the elimination of O_2^- by MnSOD is shown in Scheme 1(*21*−*23*) and can be explained assuming two concomitant pathways, both a fast

† This research was supported by BNL Laboratory Directed Research and Development Funds (D.E.C.) and NIH Grant GM 54903 (D.N.S.) and carried out at the Center for Radiation Chemistry Research at BNL, which is supported under contract DE-AC02-98CH10886 with the U.S. Department of Energy and supported by its Division of Chemical Science, Office of Basic Energy Sciences.

* Author to whom correspondence should be addressed. Tel: (+1) 631-344-4361. Fax: (+1) 631-344-5815. E-mail: cabelli@bnl.gov.

‡ Brookhaven National Laboratory.

§ University of Florida.

[1] Abbreviations: *Drad*, *Deinococcus radiodurans*; O_2^-, superoxide; MnSOD, manganese superoxide dismutases; Y34F MnSOD, site-specific mutant of MnSOD with Tyr34 replaced with Phe; PCR, polymerase chain reaction; AA, atomic absorption; FPLC, fast protein liquid chromatography; SDS−PAGE, sodium dodecyl sulfate, polyacrylamide gel electrophoresis; RPM, revolutions per minute; MeV, million electron volts.

10.1021/bi7016206 CCC: $40.75
Published on Web 02/02/2008

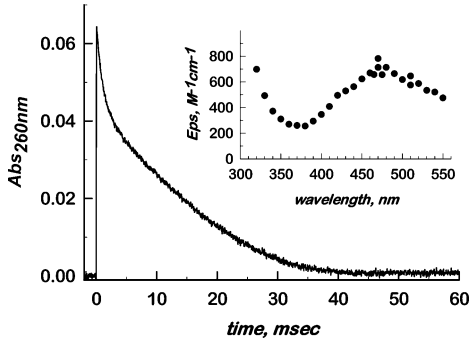

FIGURE 1: Disappearance of superoxide in the presence of *E. coli* MnSOD: 0.135 μM MnSOD, pH 7.0, 35 μM O_2^-. Inset: Spectrum of *E. coli* Mn^{3+}SOD generated when 20 μM *E. coli* Mn^{2+}SOD is reacted with 1 μM O_2^- at pH 7.0.

Scheme 1: Proposed Kinetic Mechanism for the Elimination of Superoxide by Mn-Containing Superoxide Dismutase

$$Mn^{III}SOD + O_2^{\cdot-} \xrightarrow{k_1} Mn^{II}SOD + O_2 \quad (1)$$

$$Mn^{II}SOD + O_2^{\cdot-} \xrightarrow{k_2,\ 2H^+} Mn^{III}SOD + H_2O_2 \quad (2)$$

$$Mn^{II}SOD + O_2^{\cdot-} \xrightarrow{k_3} Mn^{III}SOD\text{-}O_2^{2-} \quad (3)$$

$$Mn^{III}SOD\text{-}O_2^{2-} \xrightarrow{k_4,\ 2H^+} Mn^{III}SOD + H_2O_2 \quad (4)$$

protonation of superoxide and release of peroxide (reaction 2) and a parallel formation of an intermediate, often called the inhibited complex[2] (reaction 3) with a rate-determining protonation (reaction 4) and release of the bound peroxy moiety. In this way, the gating between the rates of the fast protonation pathway (outer sphere) and the pathway leading to an inhibited complex (inner sphere) will determine the concentration of O_2^- at which the enzymatically induced superoxide disappearance will begin to obey complex kinetic behavior (Figure 1). The actual physical process that accounts for this gating has been suggested to be isomerization between a side-on and end-on bound peroxy moiety (*23*) or a conformational change (*21*, *22*) and is thus far undefined.

The classic and most effective technique for exploring the mechanism by which different SODs dismutate O_2^- involves using pulse radiolysis, where O_2^- can be generated on a very fast time scale and its disappearance followed in the presence of varying concentrations of enzymes (*21*, *22*, *24*). In this study we have compared the O_2^- dismutation mechanisms of the *Drad*, *Escherichia coli* and human MnSODs in order to understand why *Drad* MnSOD seems to confer some additional radiation resistance onto the organism (*17*). The latter two MnSODs were chosen for comparison, as earlier studies (*25*−*27*) have suggested that they may be optimized for their individual roles in the different organisms via different gating between the inner- and outer-sphere mechanism for O_2^- reduction. We have then examined the effect upon the dismutation mechanism in *Drad* MnSOD when a tyrosine thought to be implicated in a proton-transfer relay is modified; Tyr34 to Phe34. Modification of this tyrosine has been the subject of many studies in the human and *E. coli* enzymes because the phenylalanine is completely analogous to tyrosine except for removal of a hydroxide where the OH proton takes part in a proton-transfer chain in the second sphere around the enzyme active site (*25*−*27*).

[2] The convention we will use is that the formation of a stabilized or inhibited complex is called "inner-sphere" and direct formation of peroxide is called "outer-sphere".

EXPERIMENTAL PROCEDURES

Isolation and Characterization of Drad MnSOD. Deinococcus radiodurans genomic DNA was purchased from the American Type Culture Collection (ATCC), and the desired full length MnSOD gene was amplified by PCR. The PCR product was then purified using the Promega Gel Extraction Kit and cloned into the pet31f1(−) plasmid previously digested by *Nde*I and *Bam*HI. The resulting plasmid was used to transform sodA$^-$/sodB$^-$ *E. coli* (strain QC774). *E. coli* sodA$^-$/sodB$^-$ were transformed with pTrc99A containing the *Drad* MnSOD full length sequence and grown into a large-scale culture of 2xYT media which included 1.0 mM $MnCl_2$. The bacteria were spun down and lysed (*29*). The bacterial lysate was heated to 60 °C for 10 min and centrifuged at 18,000 RPM for a 30 min. After dialysis, the lysate was loaded onto an Amersham's Hi-load 26/10 Q-Sepharose column, with high-performance resin (Amersham Pharmacia's AKTA FPLC). The protein fraction containing the *Drad* MnSOD was concentrated and the protein purity was determined using SDS−PAGE (*29*). A single intense band was observed at 22 kDa indicative of the monomer. The protein yield from 9 L of culture was 1 g. The human MnSOD was obtained as previously described (*30*), and the *E. coli* MnSOD is from Sigma. The Tyr34Phe mutant MnSOD from *Deinococcus radiodurans* was prepared following the procedures described previously (*31*).

Pulse Radiolysis Studies. The pulse radiolysis experiments were carried out using the 2 MeV Van de Graaff accelerator at Brookhaven National Laboratory. The amount of O_2^- generated during pulse-radiolysis was established using the KSCN dosimeter, assuming that $(SCN)_2^-$ has a *G* value of 6.13 and $\epsilon_{472\ nm} = 7590\ M^{-1}\ cm^{-1}$. Rates were measured by two methods: (a) generating substoichiometric O_2^- concentrations and following the disappearance or appearance of Mn^{3+}SOD at 350−650 nm as Mn^{3+}SOD has an absorbance maximum at 480 nm with an extinction coefficient of 800 $M^{-1}\ cm^{-1}$ (Figure 1, inset) or (b) following the disappearance of O_2^- at 260 nm under catalytic conditions (Figure 1), assuming the mechanism in Scheme 1 and fitting the data using the Numerical Integration of Chemical Kinetics program in PRWIN (by H. Schwarz, BNL).

Superoxide radical was generated in air-saturated aqueous solution containing sodium formate (H_2O -/\/\- → $^{\bullet}OH$, e_{aq}^-, $H^{\bullet}$, H_2, H_2O_2; $^{\bullet}OH + HCO_2^- \rightarrow CO_2^{\bullet-} + H_2O$; $e_{aq}^- + O_2 \rightarrow O_2^{\bullet-}$; $H^{\bullet} + O_2 \rightarrow HO_2^{\bullet}$; $HO_2^{\bullet} \leftrightarrow O_2^{\bullet-} + H^+$ where $K_a = 4.8$) (*32*). All adjustments to pH were carried out using sodium hydroxide and sulfuric acid. All chemicals used were of the highest purity commercially available. Mn^{3+}SOD was reduced using varying amounts of hydrogen peroxide (1:2−1:10 ratio) which has been shown to reduce the manganese center of the enzyme without loss of activity. All measurements were carried out in 10 mM phosphate buffer, 10 mM formate, 10μM EDTA at 25 °C. Under these conditions, the conversion of the primary radicals to superoxide radical was complete by the first microsecond. Enzyme and superoxide concentrations varying from 1 to 120 μM and 2 to 50 μM, respectively, were used.

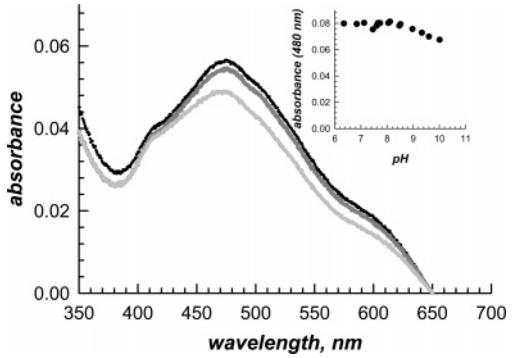

FIGURE 2: The visible absorption band of *Drad* Mn^{3+}SOD at pH 7, 9.5, and 10. Inset: The change in absorbance of *Drad* Mn^{3+}-SOD at 480 nm as a function of pH.

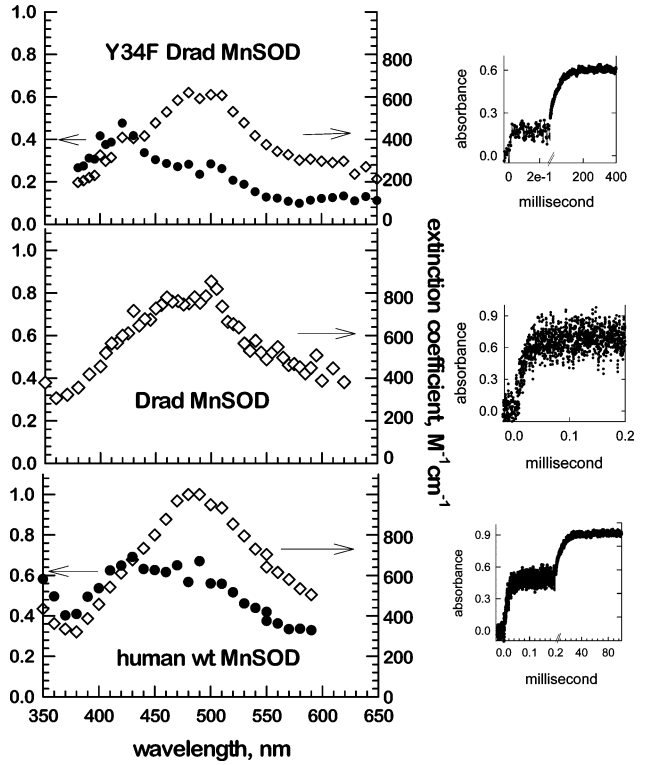

FIGURE 3: The spectra generated when O_2^- is generated in the presence of a large (at least 10-fold) excess of Mn^{2+}SOD. The final product in all cases is Mn^{3+}SOD (open diamonds). In the case of Y34F *Drad* MnSOD and human MnSOD, a transient is generated initially (closed circles) that disappears with the concomitant formation of Mn^{3+}SOD. The initial spectra (closed circles) were taken approximately 1 ms after the pulse, and the final spectra (open diamonds) were measured 100 ms after the pulse, except for *Drad* MnSOD, where no transient is observed. The change in absorbance with time at 500 nm is shown to the left of each set of spectra.

UV/vis measurements were carried out on a Cary-5 UV/vis spectrophotometer. Bimolecular rates are given relative to the total manganese concentration, and not the enzyme concentration. That serves to normalize activity for the human tetrameric enzyme and the bacterial (*E. coli* and *Dr*) dimeric enzymes. Manganese content was determined using flame atomic absorption spectroscopy. All rates are averages of at least 3 measurements with errors in the actual numbers of 5−15%, depending upon the signal-to-noise ratio (see Figure 3). The manganese concentration has an error of 15% with the caveat that any free manganese in solution is measured via AA but is not catalytically active. As the samples were extensively dialyzed, the amount of free manganese in solution is very small, but it will serve to make any calculated bimolecular rate potentially lower than the true rate. It will, of course, only affect rates that are first order in enzyme concentration. We have, therefore assumed an overall error of 15% for all the numbers and not included error bars in Table 1.

Table 1: Rate Constants for the Kinetic Mechanism of Different Mn-Containing SODs

MnSOD	k_1 (nM^{-1} s^{-1})	k_2 (nM^{-1} s^{-1})	k_3 (nM^{-1} s^{-1})	k_4 (s^{-1})
Drad	1.2	1.1	0.07	30
E. coli	1.1	0.9	0.17	60
human	1.4	0.6	0.5	130
Y34F *Drad*	0.9	0.9	0.5	30

RESULTS

The absorption band with a maximum at 480 nm for *Drad* Mn^{3+}SOD is shown in Figure 2 at three different pHs, pH 7, 9.5 and 10.0. The change in this band with pH leads to a calculated pK_a of ca. 9.5, Figure 2 inset. Both the shape of the absorption band and the pH profile are virtually identical to those found in *E. coli* Mn^{3+}SOD (*4*), further demonstrating the similarities between both of these bacterial MnSODs.

Mn^{3+}SOD can be rapidly reduced with hydrogen peroxide, whereupon the visible band disappears and the solution remains stable (*21*, *23*). The traces in Figure 3 show the spectra that result when O_2^- is generated in the presence of a large (at least 10-fold) excess of Mn^{2+}SOD. The final product in all cases is Mn^{3+}SOD (open diamonds). In the case of Y34F *Drad* MnSOD and human MnSOD, a transient is generated initially (closed circles) that disappears with the concomitant formation of Mn^{3+}SOD. This transient is written as $Mn^{3+}SOD-O_2^{2-}$ in Scheme 1, and k_4 is measured directly here from the rate of disappearance of $Mn^{3+}SOD-O_2^{2-}$ and concomitant formation of Mn^{3+}SOD. The molar extinction applies only to the final Mn^{3+}SOD absorbance as the absorption spectrum of the intermediate reflects the percentage of the initial Mn^{2+}SOD that is directly converted to Mn^{3+}SOD (reaction 2) and the percentage that is converted to $Mn^{3+}SOD-O_2^{2-}$ (reaction 3). The absorbance versus time traces that are shown to the right of the spectral data in Figure 3 were measured at 500 nm and show the actual growth of the transient and then the final Mn^{3+}SOD. Note that no transient is observed with the *Drad* MnSOD, as with the *E. coli* MnSOD (Figure 1), and the mechanism, when investigated on the substoichiometric time scale, does resemble the simple ping-pong mechanism shown for CuZnSOD.

The traces in Figure 4 show the disappearance of various concentrations of O_2^- in the presence of varying amounts of MnSOD. In panel A, the O_2^- and MnSOD are present in identical concentrations (1 μM). Here, O_2^- disappears at the same rate irrespective of whether in the presence of human MnSOD, *E. coli* MnSOD or *Drad* MnSOD. In equimolar concentrations, only k_1 or ($k_2 + k_3$) is accessed (Scheme 1), and these rate constants are identical within experimental error; see Table 1. However, under catalytic conditions, where the ratio of O_2^- to MnSOD is 10:1 (panel B), the human enzyme is already noticeably less efficient at removing O_2^-, showing an initial burst where the enzyme is cycling between superoxide oxidation (reaction 1) and superoxide reduction that involves rapid protonation off of the bound

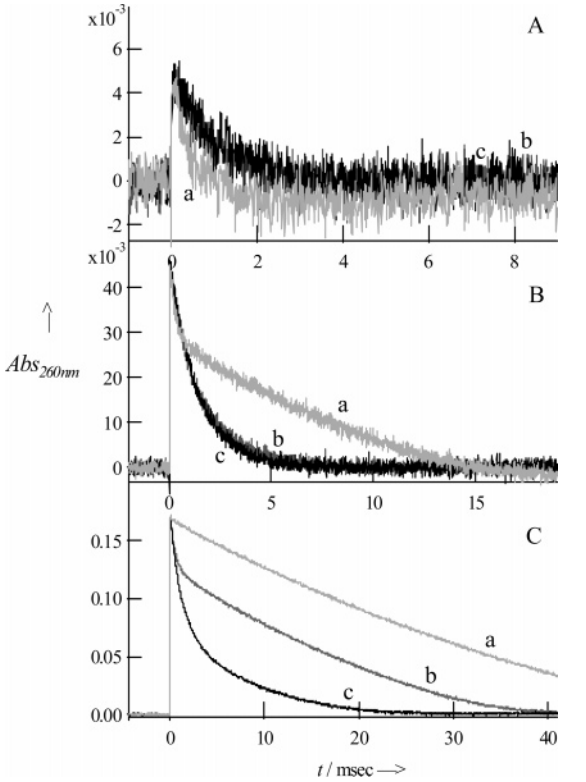

FIGURE 4: Pulse radiolysis traces for the superoxide disappearance at 260 nm. The ratios between superoxide and MnSOD are 1 in panel A (1 μM O_2^- and MnSOD), 10 in panel B (10 μM O_2^- and 1 μM MnSOD) and 41 in panel C (41 μM O_2^- and 1 μM MnSOD). (a) human MnSOD, (b) *E. coli* MnSOD, (c) *Drad* MnSOD.

peroxide (reaction 2). The burst phase is followed by a slower disappearance of the substrate in a saturation process (reaction 3) as the bound peroxo protonation and release (reaction 4) becomes rate limiting (panel B, trace A). However, when superoxide is only present in a 10-fold excess over the enzyme, both *Drad* and *E. coli* MnSODs remove that superoxide in a purely first-order catalytic fashion. In the presence of 41 μM O_2^- and 1 μM MnSOD (panel C), however, the *E. coli* and *Drad* enzymes now also induce a mechanism that involves partitioning between an inner- and outer-sphere mechanism. The dramatic difference observed here is that within 2 ms, over half the O_2^- has disappeared in the presence of *Drad* MnSOD while less than 30% has disappeared in the presence of *E. coli* MnSOD and only a few percent has disappeared in the presence of human MnSOD.

In a number of studies, it was suggested that the tyrosine, Tyr34, that is in the second sphere hydrogen-bonding network and is conserved in all of these MnSODs allows proton donation to the bound hydroxide (*33*−*35*) in the reduced MnSOD. The effect upon enzyme structure and activity when the tyrosine is mutated to phenylalanine (i.e., removal of the OH from the ring) has been studied in the human and *E. coli* enzymes. It was shown in an earlier study that when the tyrosine 34 in human wt MnSOD is mutated to phenylalanine, the enzyme loses virtually all ability to protonate off the bound peroxy moiety in a fast process and catalysis becomes limited by exclusive use of the slow protonation pathway (*33*). In light of this, it was of interest to make the Y34F *Drad* MnSOD in order to query the role of the tyrosine in this very efficient dismutase. As seen in

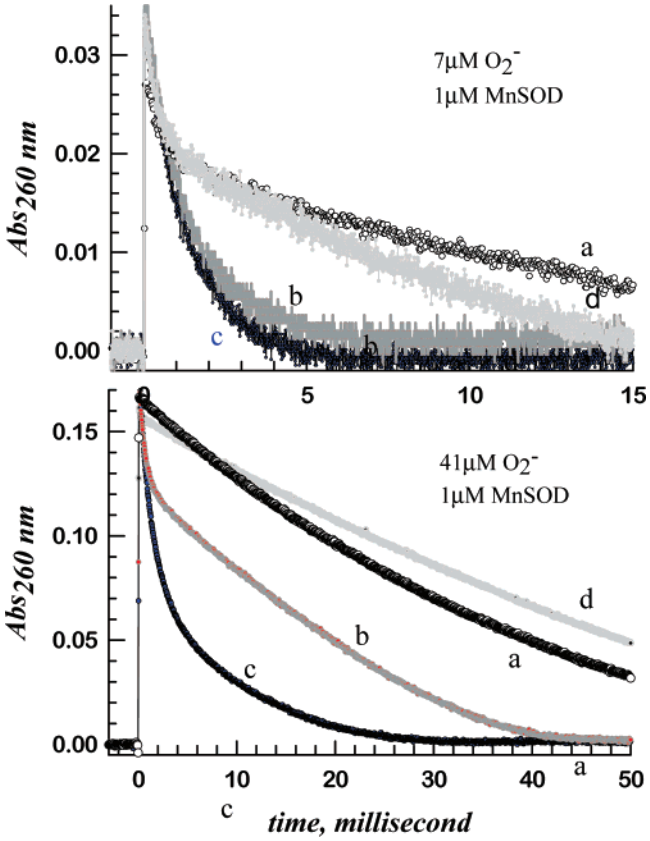

FIGURE 5: Pulse radiolysis traces for the superoxide disappearance at 260 nm. The ratios between superoxide and MnSOD are 1:7 in top panel (7 μM O_2^- and 1 μM MnSOD) and 1:41 in bottom panel (41 μM O_2^- and 1 μM MnSOD). (a) Human MnSOD, (b) *E. coli* MnSOD, (c) *Drad* MnSOD, (d) Y34F *Dr*MnSOD.

Figure 3, when the *Drad* Mn^{2+}SOD reacts with a substoichiometric amount of superoxide, *Drad* Mn^{3+}SOD is produced (with an absorbance maximum at 480 nm). No evidence is seen of any transient, corroborating that reaction 2 is favored over reaction 3. In contrast, when human Mn^{2+}-SOD is interrogated with substoichiometric amounts of superoxide, an immediate spectrum is formed that has absorbances at both 480 and 420 nm, attributed to simultaneous direct formation of human Mn^{3+}SOD and human Mn^{3+}SOD$-O_2^-$ adduct, respectively. Then, at a slower, first-order rate, the peroxo-adduct is protonated and loses the bound peroxide. The magnitudes of the two absorbances suggest the two pathways occur at similar rates, in agreement with the measurements carried out at 260 nm discussed previously. When the *Drad* Y34F Mn^{2+}SOD is reacted with substoichiometric superoxide, the resultant kinetic behavior is similar to that of human MnSOD, not *Drad* MnSOD.

This is further corroborated in studies using high concentrations of superoxide in the presence of *Drad* Y34FMnSOD; Figure 5. Here, the traces for the *Drad* Y34F MnSOD are plotted on the previously shown traces (Figure 4). As is apparent, the disappearance of superoxide with time in the presence of *Drad* Y34F MnSOD is now virtually superimposable with the analogous study in the presence of human MnSOD. These studies at two different ratios of superoxide: MnSOD and the results were consistent under both conditions and in agreement with the studies described previously using substoichiometric superoxide.

DISCUSSION

This uniquely efficient ability of *Drad* MnSOD to remove high concentrations of O_2^- may be physiologically relevant since the high level of radiation *Drad* can endure will enhance the intracellular ROS concentration. In fact, the difference between this enzyme and the MnSODs studied previously is not that this enzyme reacts with O_2^- at a faster rate but that the reductase step (reactions 2 and 3) partitions toward an outer-sphere mechanism rather than an inner-sphere or saturative mechanism.

The differences in the reactivity of the enzymes are then a direct result of their k_2/k_3 ratio; the human enzyme has a $k_2/k_3 \approx 1$, while in the *E. coli* SOD this ratio is close to 5 (obtained from Table 1), favoring an outer-sphere mechanism. Several point mutations in the human MnSOD have been made to try to alter the gating between k_2 and k_3 and so far have failed in the task of making the human enzyme more *E. coli*-like (*19*). Instead, many of these mutations simply shut down the catalytic cycle (reactions 1 and 2), making the reaction of the reduced form of the enzyme occur exclusively through an inhibited complex (*18*). *Drad* MnSOD is a more efficient enzyme than *E. coli* in dealing with high O_2^- concentrations as the k_2/k_3 ratio (*ca.* 16) is even greater than the one for the *E. coli* enzyme.

It is interesting that the human and *E. coli* MnSODs share a 41% similarity in their amino acid sequence (*24*) while the primary sequences of the MnSODs from *E. coli* and *Drad* show a much higher degree of similarity (68%); the main difference being a small insert (Q92 to A97) in the *Drad* enzyme. Since the latter enzymes show similar catalytic activity rates, the features controlling the gating between k_2 and k_3 remain to be identified. The crystal structures of all three enzymes are known, with the publishing of the *Drad* MnSOD structure (*39*). All three structures show a high degree of similarity around the active site, with the interesting feature that the human MnSOD is a tetramer while the two bacterial MnSODs are dimers. Clearly, the dimer−tetramer interface is a promising area to probe. Some answers may arise from a careful comparison of the crystal structures of all three enzymes in that region.

An interesting question arises as to the efficiency of *Drad* and *E. coli* cells at H_2O_2 elimination. The human enzyme can only deal efficiently with lower O_2^- concentrations than the *E. coli* MnSOD (*24*). Apparently, in the eukaryotic enzyme, the release of a high concentration of H_2O_2 is avoided. This can be viewed as part of the complex system to keep a highly regulated steady-state concentration of peroxide as slight changes in H_2O_2 concentration have been proposed to determine whether H_2O_2 acts to induce processes as varied as cell proliferation to apoptosis (*37*, *38*). In fact, a recent proposal has suggested that MnSOD acts in human cells to maintain a specified reducing gradient (*38*). If, in human cells, MnSOD is designed to avoid an excess efflux of H_2O_2 to the cell, this capability is not essential to *Drad*, because here the concentration of H_2O_2 is not as crucial or/and this organism may have a very efficient way to eliminate it. That a *kat A* mutant of *Drad* shows no difference in radiation sensitivity (*10*) suggests that either the remaining defenses against hydrogen peroxide are adequate or peroxide in this enzyme is not as toxic as in other less radiation resistant cells. This question is an exciting avenue for future research.

Scheme 2: Cartoon Illustrating the Differences Observed in Wild Type MnSODs from Various Organisms and Modified Human and *Drad* MnSODs

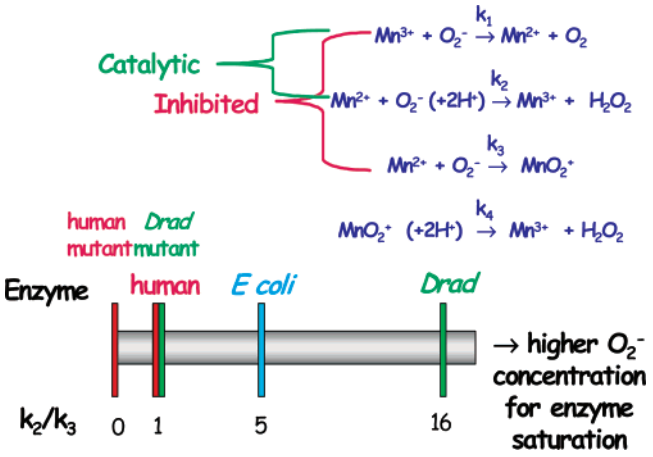

CONCLUSION

We show here that *Drad* MnSOD is able to efficiently eliminate higher O_2^- concentrations than MnSODs in other organisms. This results not from an accelerated rate of interaction between the superoxide radical and the enzyme but rather from a mechanism that favors rapid protonation off of the bound peroxide from the oxidized metal over a slower protonation process. That MnSODs seem to dismutate superoxide via a mechanism that involves two different pathways, a slow protonation off of superoxide and a fast protonation off of superoxide, is quite unique. Further, that this mechanism shows kinetic variability over different organisms, specifically human, *E. coli* and *Drad*, leads to the obvious question of whether there is an evolutionary driver for these observed differences. The evidence that is accumulating seems to suggest that these kinetic differences show a pattern. We would like to suggest a mechanism that involves the interplay between the efficient superoxide removal and less efficient peroxide production. In particular, the very rapid removal of superoxide in *Drad* suggests that the removal of superoxide is paramount, regardless of production of peroxide. In contrast, the remarkably slow removal of superoxide in the human enzyme at elevated superoxide concentrations, coupled with the tumoricidal effects shown in cell and mouse studies with an engineered efficient human MnSOD (*36*), suggests, conversely, that the rate of peroxide production may be significant in human cells as a signaling agent. In fact, in human cells, the rate of peroxide production may be as crucial as the rate of superoxide removal (*37*, *38*).

This suggested mechanism is based on our existing database of MnSODs. Pulse radiolysis studies of MnSODs from *Thermus thermophilus* (*23*) and *Bacillus stearothermophilus* (*21*) suggest a kinetic behavior similar to that of *E. coli* MnSOD, not surprising as they are also bacterial MnSODs. Clearly, the kinetic behavior of MnSODs from other organisms such as yeast, *C. elegans* and various insects may be of great interest, and these questions are being actively pursued. The final fascinating feature is that shown in Scheme 2, that mutants made thus far of the human

enzyme only serve to make an enzyme that favors a slow protonation pathway and the mutant of *Drad* only served to remove most of the fast protonation pathway and turn the enzyme into one where the kinetics resemble that of the human enzyme. The recently published dimeric structure of *Drad* MnSOD (*39*) clearly suggests that dimer versus tetramer structure may be as significant to protonation as modification of residues in the second sphere and modification of the purported proton-transfer pathway. However, the reversion of *Drad* Y34FMnSOD to a kinetic behavior similar to that of human MnSOD indicates an incomplete understanding of the structural differences that lead to the different kinetic pathways.

The use of *Drad* is being actively pursued for bioremediation purposes so an understanding of the biochemistry that may lead any amount of radiation resistance becomes very important. Perhaps even more importantly, the understanding of the mechanism in MnSOD and its physiological implications in different organisms can lead to the construction of better therapeutic SOD-like synthetic compounds that can be used in the protection against the deleterious effects of treatments like radiotherapy.

ACKNOWLEDGMENT

The authors gratefully acknowledge Dr. Morris Bullock for valuable discussions.

REFERENCES

1. Battista, J. R. (1997) Against all odds: the survival strategies of Deinococcus radiodurans, *Annu. Rev. Microbiol. 51*, 203−224.
2. White, O., Eisen, J. A., Heidelberg, J. F., Hickey, E. K., Peterson, J. D., Dodson, R. J., Haft, D. H., Gwinn, M. L., Nelson, W. C., Richardson, D. L., Moffat, K. S., Qin, H., Jiang, L., Pamphile, W., Crosby, M., Shen, M., Vamathevan, J. J., Lam, P., McDonald, L., Utterback, T., Zalewski, C.,. Makarova, K. S., Aravind, L., Daly, M. J., Minton, K. W., Fleischmann, R. D., Ketchum, K. A., Nelson, K. E., Salzberg, S., Smith, H. O., Venter, J. C., and Fraser, C. M. (1999) Genome sequence of the radioresistant bacterium Deinococcus radiodurans R1, *Science 286*, 1571−1577.
3. Levin-Zaidman, S., Englander, J., Shimoni, E., Sharma, A. K., Minton, K. W., and Minsky, A. (2003) Ringlike structure of the Deinococcus radiodurans genome: a key to radioresistance?, *Science 299*, 254−256.
4. Battista, J. R., Cox, M. M., Daly, M. J., Narumi, I., Radman, M., and Sommer, S. (2003) The structure of D. radiodurans, *Science 302*, 567.
5. Minsky, A., Sharma, A. K., and Englander, J. (2003) Response, *Science 302*, 567−568.
6. Daly, M. J., Gaidamakova, E. K., Matrosova, V. Y., Vasilenko, A., Zhai, M., Venkateswaran, A., Hess, M., Omelchenko, M. V., Kostandarithes, H. M., Makarova, K. S., Wackett, L. P., Fredrickson, J. K., and Ghosal, D. (2004) Accumulation of Mn(II) in Deinococcus radiodurans facilitates gamma-radiation resistance, *Science 306*, 1025−1028.
7. Ghosal, D, Omelchenko, M. V., Gaidamakova, E. K., Matrosova, V. Y., Vasilenko, A., Venkateswaran, A., Zhai, M., Kostandarithes, H. M., Brim, H., Makarova, K. S., Wackett, L. P., Fredrickson, J. K., and Daly, M. J. (2005) How radiation kills cells: survival of Deinococcus radiodurans and Shewanella oneidensis under oxidative stress, *FEMS Microbiol. Rev. 29*, 361−367.
8. Zahradka, K., Slade, D., Bailone, A., Sommer, S., Averbeck, D., Petranovic, M., Lindner, A. B., and Radman, M. (2006) Reassembly of shattered chromosomes in Deinococcus radiodurans, *Nature 443*, 569−573.
9. Hua, Y., Narumi, I., Gao, G., Tian, B., Satoh, K., Kitayama, S., and Shen, B. (2004) PprI: a general switch responsible for extreme radioresistance of Deinococcus radiodurans. (2003), *Biochem. Biophys. Res. Commun. 306*, 354−360.
10. Narumi, I., Satoh, K., Cui, S., Funayama, T., KitayamaS., and Watanabe, H. (2004) PprA: a novel protein from *Deinococcus radiodurans* that stimulates DNA ligation, *Mol. Microbiol. 54*, 278−285.
11. Tanaka, M., Earl, A. M., Howell, H. A., Park, M.-J., Eisen, J. A., Peterson, S. N., and Battista, J. R. (2004) Analysis of *Deinococcus radioduran's* Transcriptional Response to Ionizing Radiation and Dessication Reveals Novel Proteins That Contribute to Extreme Radioresistance, *Genetics 168*, 21−33.
12. Blasius, M., Shevelev, I., Jolivet, E., Sommer, S., and Hubscher, U. (2006) DNA polymerase X from *Deinococcus radiodurans* possesses a structure-modulated 3′→5′ exonuclease activity involved in radioresistance, *Mol. Microbiol. 60*, 165−176.
13. Zhang, C., Wei, J., Zheng, Z., Ying, N., Sheng, D., and Hua, Y. (2005) Proteomic Analysis of Deinococcus radiodurans recovering from γ-irradiation, *Proteomics 5*, 138−143.
14. Cox, M. M., and Battista, J. R. (2005) Deinococcus Radiodurans—The Consummate Survivor, *Nat. Rev. Microbiol. 3*, 882−892.
15. Earl, A. M., Mohundro, M. M., Mian, I. S., and Battista, J. R. (2002) The IrrE protein of Deinococcus radiodurans R1 is a novel regulator of recA expression, *J. Bacteriol. 184*, 6216−6224.
16. Kobayashi, I., Tamura, T., Sghaier, H., Narumi, I., Yamaguchi, S., Umeda, K., and Inagaki, K. (2006) Characterization of monofunctional catalase KatA from radioresistant bacterium deinococcus radiodurans, *J. Biosci. Bioeng. 101*, 315−321.
17. Markillie, L. M., Varnum, S. M., Hradecky, P., and Wong, K.-K. (1999) Targeted mutagenesis by duplication insertion in the radioresistant bacterium Deinococcus radiodurans: radiation sensitivities of catalase (katA) and superoxide dismutase (sodA) mutants, *J. Bacteriol. 181*, 666−669.
18. Juan J. Y., Keeney, S. N., and Gregory, E. M. (1991) Reconstitution of the Deinococcus radiodurans aposuperoxide dismutase, *Arch. Biochem. Biophys. 286*, 257−263.
19. Yun, Y. S., and Lee, Y. N. (2003) Production of Superoxide Dismutase by *Deinococcus radiophilus*, *J. Biochem. Mol. Biol. 36*, 282−287.
20. Yun, Y. S., and Lee, Y. N. (2004) Purification and some properties of superoxide dismutase from *Deinococcus radiophilus*, the UV-resistant bacterium, *Extremophiles 8*, 237−242.
21. McAdam, M. E., Fox, R. A., Lavelle, F., and Fielden, E. M. (1977) A pulse-radiolysis study of the manganese-containing superoxide dismutase from Bacillus stearothermophilus. A kinetic model for the enzyme action, *Biochem. J. 165*, 71−79.
22. Pick, M., Rabani, J., Yost, F., and Fridovich, I. (1974) Catalytic mechanism of the manganese-containing superoxide dismutase of Escherichia coli studied by pulse radiolysis, *J. Am. Chem. Soc. 96*, 7329−7333.
23. Bull, C., Niederhoffer, E. C., Yoshida, T., and Fee, J. A. (1991) Kinetic studies of superoxide dismutases: properties of the manganese-containing protein from Thermus thermophilus, *J. Am. Chem. Soc. 107*, 3295.
24. Cabelli, D. E., Riley, D., Rodriguez, J. A., Valentine, J. S. and Zhu, H. (2000) Models of Superoxide Dismutases, in *Biomimetic Chemistry* (Meunier, B., Ed.) A, pp 461−508, Imperial College Press, London.
25. Hearn, A. S., Stroupe, M. E., Cabelli, D. E., Lepock, J. R., Tainer, J. A., Nick, H. S., and Silverman, D. N. (2001) Kinetic analysis of product inhibition in human manganese superoxide dismutase, *Biochemistry 40*, 12051−12058.
26. Cabelli, D. E., Guan, Y., Leveque, V., Hearn, A. S., Tainer, J. A., Nick, H. S., and Silverman, D. N. (1999) Role of tryptophan 161 in catalysis by human manganese superoxide dismutase, *Biochemistry 38*, 11686−11692.
27. Leveque, V., Stroupe, M. E., Lepock, J. R., Cabelli, D. E., Tainer, J. A., Nick, H. S., and Silverman, D. N. (2000) Multiple replacements of glutamine 143 in human manganese superoxide dismutase: effects on structure, stability, and catalysis, *Biochemistry 39*, 7131−7137.
28. Beck, Y., Bartfeld, D., Yavin, Z., Levanon, A., Gorecki, M., and Hartman, J. R. (1988) Efficient Production of Active Human Manganese Superoxide-Dismutase in Escherichia-Coli, *Bio/Technology 6*, 930−935.
29. Laemmli, U. K. (1970) Cleavage of structural proteins during the assembly of the head of bacteriophage T4, *Nature 227*, 680−685.
30. Hsu, J.-L., Hsieh, Y., Tu, C., O'Connor, D., Nick, H. S., and Silverman, D. N. (1996) Catalytic properties of human manganese superoxide dismutase, *J. Biol. Chem. 271*, 17687−17691.

31. Guan, Y., Hickey, M. J., Borgstahl, G. E. O., Hallewell, R. A., Lepock, J. R., O'Connor, D., Hsieh, Y., Nick, H. S., Silverman, D. N., and J. A. Tainer (1998) Crystal Structure of Y34F Mutant Human Mitochondrial Manganese Superoxide Dismutase and the Functional Role of Tyrosine 34, *Biochemistry 37*, 4722−4730.
32. Schwarz, H. A. (1981) Free radicals generated by Radiolysis of Aqueous Solutions, *J. Chem. Educ. 58*, 101−105.
33. Abreu, A. I., Rodriguez, J. A., and Cabelli, D. E. (2005) Theoretical studies of manganese and iron superoxide dismutases: superoxide binding and superoxide oxidation, *J. Phys. Chem. B 109*, 24502−24509.
34. Hearn, A. S., Stroupe, M. E., Cabelli, D. E., Ramilo, C. A., Luba, J. P., Tainer, J. A., Nick, H. S., and Silverman, D. N. (2003) Catalytic and structural effects of amino acid substitution at histidine 30 in human manganese superoxide dismutase: insertion of valine C gamma into the substrate access channel, *Biochemistry 42*, 2781−2789.
35. Maliekal, J., Karapetian, A., Vance, C., Yikilmaz, E., Wu, Q., Jackson, T., Brunold, T. C., Spiro, T. G., and Miller, A.-F. (2002) Comparison and Contrasts between the Active Site PKs of Mn-Superoxide Dismutase and Those of Fe-Superoxide Dismutase, *J. Am. Chem. Soc. 124*, 15064−15075.
36. Davis, C. A., Hearn, A. S., Fletcher, B., Bickford, J., Garcia, J. E., Leveque, V., Melendez, J. A., Silverman, D. N., Zucali, J., Agarwal, A., and Nick, H. S. (2004) Potent anti-tumor effects of an active site mutant of human manganese-superoxide dismutase. Evolutionary conservation of product inhibition, *J. Biol. Chem. 279*, 12769−12776.
37. Policastro, L., Molinari, B., Larcher, F., Blanco, P., Podhajcer, O. L., Costa, C. S., Rojas, P., and Duran, H. (2004) Imbalance of antioxidant enzymes in tumor cells and inhibition of proliferation and malignant features by scavenging hydrogen peroxide, *Mol. Carcinog. 39*, 103−113.
38. Buettner, G. R., Ng, C. F., Wang, M., Rodgers, V. G., and Schafer, F. Q. (2006) A new paradigm: manganese superoxide dismutase influences the production of H_2O_2 in cells and thereby their biological state, *Free Radical Biol. Med. 41*, 1338−1350.
39. Dennis, R. J, Micossi, E., McCarthy, J., Moe, E., Gordon, E. J., Kozielski-Stuhrmann, S., Leonard, G. A., and McSweeney, S. (2006) Structure of the manganese superoxide dismutase from Deinococcus radiodurans in two crystal forms, *Acta Crystallogr., Sect. F: Struct. Biol. Cryst. Commun. 62*, 325−329.

BI7016206